Stability Analysis of Cold-Emission Cathodes with Epoxy Coating

A. Knápek[1], L. Grmela[1]
[1] Department of Physics, FEKT VUT v Brně,
Technická 8, Brno
E-mail: alexandr.knapek@phd.feec.vutbr.cz, grmela@feec.vutbr.cz

Abstract:

In this paper, the current stability analysis was performed on the cold-emission cathode covered by a thin epoxy film. Non-destructive spectroscopic method, which is based on measuring current fluctuations, has been used to determine cathodes' quality, which directly influents the stability of the emission current. Our investigations have been performed on tungsten cathodes with extra-sharp nanotip, operating under the HV (high-vacuum) conditions, usually in vacuums of 10^{-5} Pa order. All the cathodes used for this experiment have been prepared in our lab by improved electrochemical etching method, which is based on the presence of increased surface tension allowing reaching the geometrically precise shape of the cathodes' tip. After the two phase etching method, the tip was cleared and covered by thin epoxy film, which prevents the tip to be destroyed by ion bombardment that is caused by ions attracted back on to the cathode surface. A comprehensive investigation was carried out to determine particular noise sources and to compare clean cathodes with the resin-coated one, in order to describe the influence of the oxide and dielectric epoxy layer on to the emission current stability. Spectra obtained, for various emission currents at different voltages, are described and explained. The results suggest that the resin-layer changes cathode performance and extends its durability.

INTRODUCTION

The analysis of charge carrier transport in polymer insulating layer covered by polymer layer was performed at temperature 300 K. The main goal of our research is to assess the parameters of the band diagram MIS structure [1], [2], [3] and [6].

Insulating films always contain impurities like oxygen vacancies and traps. These impurities form localized states for charge carriers in the forbidden energy gap. When the localized electronic wave functions of the localized states overlap, an electron bound to one impurity state can tunnel to an unoccupied state without involving activation into the conduction band. This tunneling process between impurity sites is referred to as impurity conduction.

The mobility of an electron moving through impurity states is small especially at low temperatures. Then, the conduction mechanism is mainly influenced by electron hopping between neighboring impurity site. This type of the conduction process depends on impurity concentration and the energy depths of the impurity states. The concept of the hopping transport has been used for a long time in connection with ionic conduction; ions move essentially by hopping, whether through interstices or vacancies.

TUNNELING CURRENT

The emission current is at low temperatures and high electric fields mainly influenced by electron tunneling through a potential barrier. Electron tunnelling through thin insulating layer is a quantum effect in which electron is considered as a wave. Wavelength of electron moving with average thermal velocity $v_{th} = 10^5$ m/s is $\lambda = h/m_e v_{th} \sim 1$ nm, where h is Planck constant, $m_e v_{th}$ is electron momentum.

Current can be described as electron traveling wave with an amplitude A_1 in cathode and amplitude A_2 in the conduction band of polymer insulating layer (see Fig. 1.). The wave amplitude exponentially decreases with the thickness t of the potential barrier between cathode and insulating layer. The energy of the electron and the electron wave length λ are assumed to be constant during the transport. The barrier high U_0 depends on the work function W_a or W_c of the anode or cathode material and the electron affinity of the insulating layer (the epoxy coating). Schematic representation of quantum tunneling for a triangular potential barrier is shown in Fig 1, where W is electron total energy and $\Delta e\Phi_B$ is the Schottky barrier lowering. For electric field intensity E = 1 mV/cm this value is $\Delta e\Phi_B$ = 60 meV for electron tunneling from cathode to insulating layer.

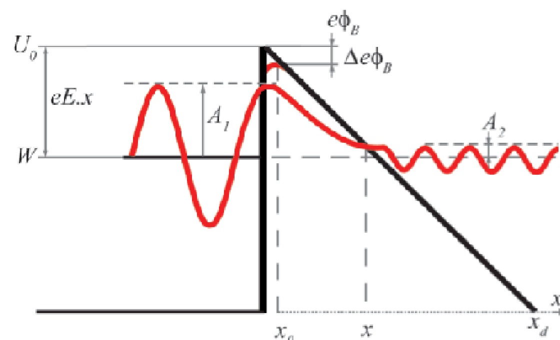

Figure 1. Schematic representation of quantum tunneling through the triangular potential barrier

For the tunneling probability D it holds [2]

$$D = D_0 \exp\left(-\frac{4\pi}{h} \int_0^{X_d} \sqrt{2m^*} \sqrt{U - W}\, dx \right) \qquad (1)$$

where D_o is constant and in first approximation D_o= 1, x_d is the insulating layer thickness, m^* is effective electron mass, h = 6.6x10^{-34} Js is Planck constant and U is the barrier energy and W is electron total energy. After integration we have for tunneling probability:

$$D = D_0 \exp\left(-\frac{8\pi\sqrt{2m^*}(e\phi_B)^{3/2}}{3ehE} \right) \qquad (2)$$

It is important that tunneling is in first approximation temperature independent and then from experiment in low temperature the barrier high can be estimated for given value of effective electron mass. For the tunneling current density J vs. electric field strength E one can write [1]

$$J = G_T E^2 \exp\left(-\frac{E_T}{E} \right) \qquad (3)$$

where G_T and E_T are the tunneling current density constants. The tunneling parameter E_T can be expressed for the energy barrier eΦ_o as

$$E_T = \frac{8\pi\sqrt{2m^*}}{3eh}(e\Phi_0)^{1.5}. \qquad (4)$$

The value of tunneling current depends on the electron effective mass and then the potential barrier energy $e\Phi_0$ (in eV) vs. tunneling parameter E_T

CATHODE FABRICATION

Basic review, of various etching methods intended for the sharp-tip cathode fabrication, was published in 1991 by Melmed [7]. All of these methods are based on the same principles.

In our experiment, we took the advantage of computer processing, and let whole etching process, to be driven and analyzed in real time. Whole process of sample manufacture was designed and driven from the Matlab, which offers comfort instrument programming without the need of accession to low level functions of used instruments.

Basically, the etched metal wire is inserted in to a grounded cylinder which is filled with a liquid electrolyte. The etching procedure is then processed in the cylinder where the etched wire acts like an anode during the process of anodic dissolution. The name of the method (drop-off) is derived from the bottom part of the etched wire which drops-off (down) during the etching procedure. The curvature radius of the tip apex, at the moment of the drop-off, can be expressed as [8]:

$$r = R\sqrt{(\rho_w - \rho_e)L/\sigma} \qquad (5)$$

where the R and L are the dropping part radius or length, σ is the ultimate tensile strength and ρ_w and ρ_e are the tungsten and electrolyte densities. This means that the resulting tip sharpness depends on the dropping part dimensions which should be as small as possible (see Fig. 2). Small mass of the dropping part minimizes some negative effects connected with sudden release of the stored elastic energy when the wire is broken. If the energy release increases to high value, it may cause the tips to recoil, melt or bend causing blunting and tip apex deformation [8].

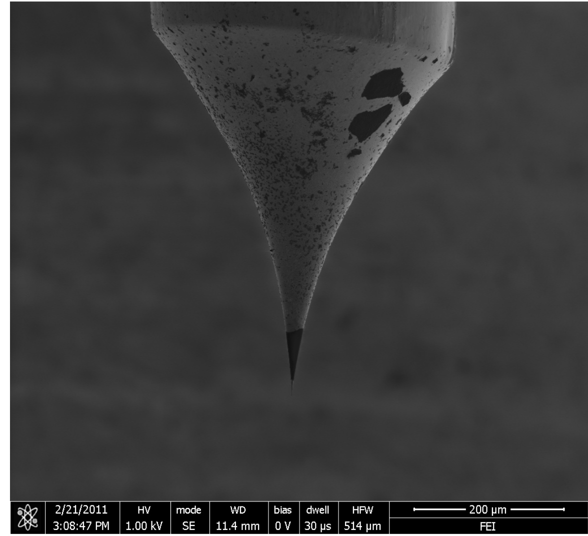

Figure 2. Manufactured sample cathode, with the epoxy coating. Note the surface impurities caused by presence of carbon

Usually the initial length of the wire, immersed in to a solution, is used as the parameter determining the length of the drop-off part. If the wire is not completely immersed, this leads to complete tip dissolution whereas if the wire is immersed too deeply, it leads to the premature neck breaking. In both cases, the sharpness of the fabricated tip becomes blunt. After the electrochemical etching process the tip is unavoidable covered by a residual layer of tungsten oxides and with other contaminants (hydrocarbons and carbides for example).

While the tip apex sharpness dependent on the electrochemical etching, the tips clarity determines its effort. For the cathode fabrication, polycrystalline tungsten wire with the diameter of 0.2mm immersed in the solution of NaOH was used. The NaOH solution was present in two molar concentrations (2M and 0.2M) for the first and second etching phase.

The laboratory fabrication consists of eight basic steps which are described further in the text.

1. Step - mechanical cleaning of the wire - the wire is cleaned by the abrasive paper of high granularity (2000 gr/cm^2) which removes surface oxide layers.

2. Step - electrochemical cleaning of the wire - before the first etching phase, the wire is cleaned by the AC current of defined frequency and amplitude which makes the surface smooth and improves its wettability.

3. Step - electrolyte surface detection and wire immersion on to the surface - during the wire immersion, the current value is continually measured and in the moment of reaching defined value, the micrometric lifter stops. By this method we can set the position of the wire exactly on the solution's surface (fig. 3.a).

4. Step – the first etching phase - in this phase the immersed wire is etched in the 20% solution of NaOH and connected to the DC voltage of 6.9V. The first phase runs until the current threshold is reached (usually around 3.5mA). After first phase the wire thins near the surface. Here the etching runs faster thanks to the surface tension which is pressing the tungsten wire. (fig. 3.b)

5. Step - resetting the wires position - this is the most critical part of whole fabrication. The constricted region must be set 0.2mm higher under the solution surface. The surface tension makes the final shape of the tip apex and leads to the drop-off of the wires bottom part. (fig. 3.c)

6. Step – the second etching phase - in this phase, the final tip shape is prepared. Etching takes place in the 5% solution of NaOH with exponentially lowering voltage which is continually set up by the computer. Lowering the voltage lowers current density before the tip is drawn up from the solution. (fig. 3.d)

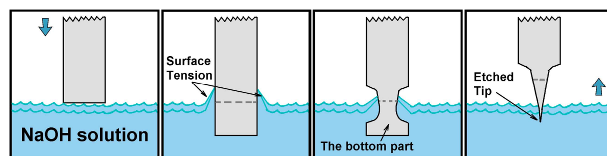

Figure 3. Etching procedure: a) immersing tungsten wire in to the electrolyte b) surface tension forming the tip geometry during etching c) bottom part starts to separate d) bottom part drops off

7. Step – the drop-off detection - during the etching, the current values are continually measured and saved after discrete time intervals. In exact current range, the drop-off detector is activated waiting for the rapid current decrease which occurs just after the bottom part drops off.

8. Step - additional technological steps - these steps are implemented in order to reach the required clearance and to increase the tip's chemical immunity. Firstly the tip is immersed in to the distilled water in order to remove solution residuals. Then the tip is immersed in to the chloroform to remove rest of carbon contaminants, which are present in the tungsten wire, because of the manufacture technology. Finally, the tip is covered by the thin epoxy coating, heated (to finish the polymerization) and placed in the vacuum chamber in order the measurement could be performed.

The moving part of the etching installation was made of micrometric stepper motor controlled device which allowed us to perform defined reproducible movements. The static part of the etching installation contained the chemically resistant cylinder made of corrosion-proof steel in which the liquid solution was located, however Petri plate with immersed steel electrode can be used as well.
For the ultra-sharp cold-cathode tip fabrication, the tungsten wire immersed in to the NaOH solution, carries an electron flow (less than 10 mA) under the voltage of 6.9V. Both the anode (tungsten wire) and the cathode (steel cylinder) were connected to the precise DC voltage laboratory power source. The current owing through the wire was changing according to the thickness of the tungsten wire. The current value decreases as the wire becomes thinner, (in the range of miliamperes to the approximately 50 microamperes) when the bottom part drops off.

MEASUREMENT METHOD

The cathode was tested in two-stage vacuum chamber, under the high-vacuum (HV) conditions, when the pressure was about $2\cdot10^{-5}$ Pa (see Fig. 8). This level of vacuum was reached by common means of turbo-molecular pump and ion pump, which are able to reach such a quality vacuum. The extraction voltage was set to -5000 V.

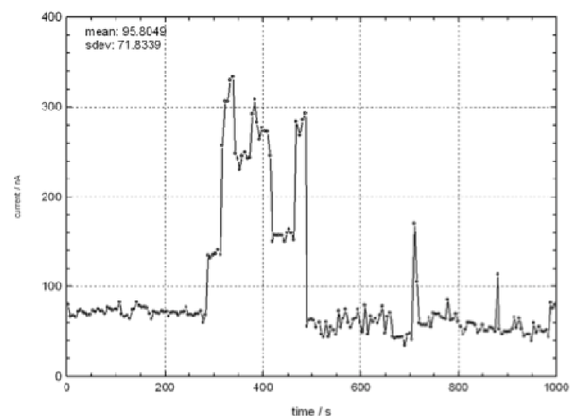

Figure 4. Emission current mean value and standard deviation intime at the beginning of cathode lifetime

The acceleration voltage was manually increased to the level, where the noise trace became apparent. Immediately, after the electron beam appeared on the faceplate (green spot), the cathode's noise characteristic was recorded. Each of the realization took 8 minutes and during this period, 80.000 samples were recorded.

Recently, it has been pointed out many times to the presence of the emission current fluctuations, occurring in the investigated structure that causes electrical noise on both thermionic and on cold or Schottky cathodes. Together with the chemical activation, which is connected to work function level change, there is also relation to the noise properties of the particular cathode. For the cold emission cathodes, the prevailing noise component originates from the local changes on the cathode surface, because of surface inhomogenities, that affects work function.

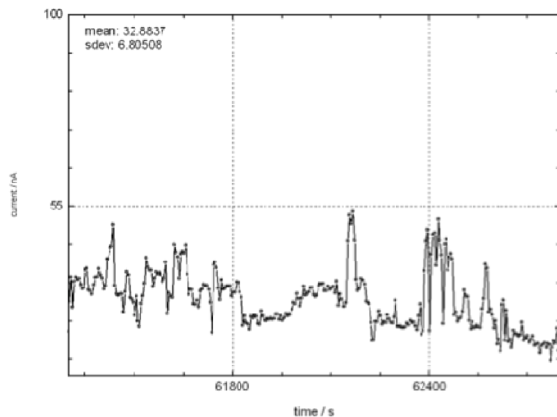

Figure 5. Emission current mean value and standard deviation in time on short before its end

Current fluctuations, caused by these changes, have significant amplitude (until 30%) and low frequency, especially for cathodes working under the room temperature, where frequencies decrease < 1 Hz.

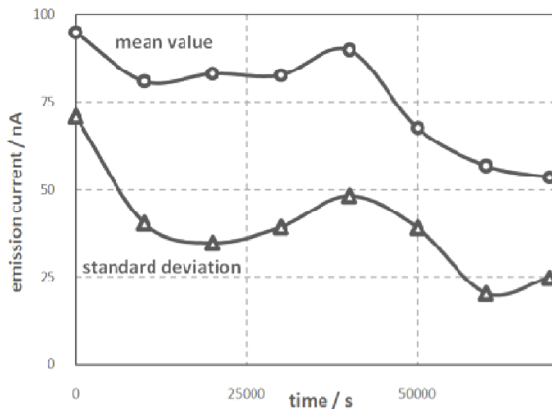

Figure 6. Current mean value and standard deviation in time

Only limited amount of atoms is taking place in the emission process (about hundreds of atoms) and adsorption of next few electrons causes significant change of the work function.

Figure 6. summarizes long-time noise measurement, which was performed on the cold emission cathode sample for 24 hours. The measurement results suggest presence of diffusion, which is evident from the mean value and standard deviation in time. The emission current is slowly increasing, that is caused by ion movement. Ions are moving inside and causing creation of spatial charge, which has essential influence on the charge transport. During this process, so called the defect band, which is located approximately 0.8eV under the electron affinity level, is created.

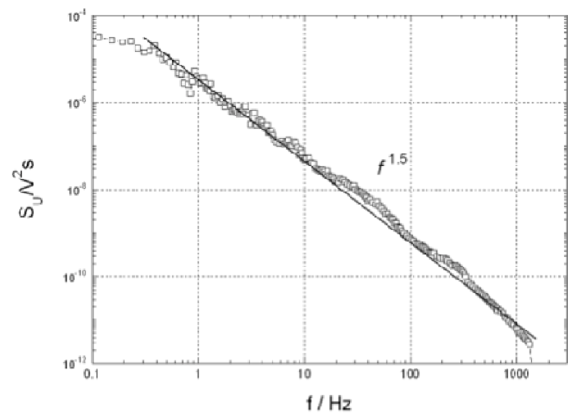

Figure 7. Power spectral density of the emission current in lower part of the frequency spectra

Figure 7 deals with the spectral analysis of the emission current. On the basis of reached results, it is evident that measured noise has characteristics of so called $1/f$ (flickering) noise.

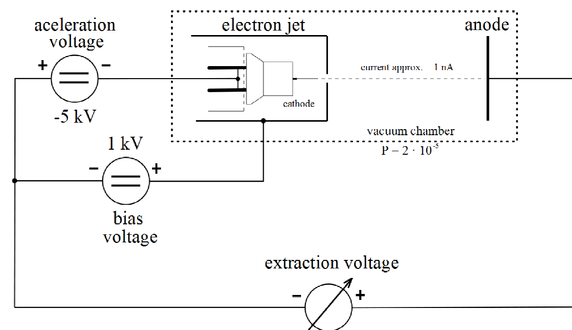

Figure 8. Cold emission cathode measurement set-up (placed in the vacuum chamber)

The $1/f$ noise is a process with a frequency spectrum such that the power spectral density is proportional to the reciprocal of the frequency. The 1/f n noise (where n > 1) originates from the superposition of particular 1/f and generation-recombination (G-R) processes, which originates from adsorption and

desorption of various atoms belonging among residual gas in the vacuum chamber.

CONCLUSIONS

The experimental fabrication resulted in creation of active Schottky cathodes with very sharp tip (fig. 2) using the computer controlled electrochemical etching technique. This method can be extended for other metal wires as well. Anodic oxidation, used to prepare thick oxide layers with thicknesses of about 30 to 100nm, can be modified further to achieve the optimal value of tunneling current.

Our research shows that the isolation coating-layer has to be as thin as possible, in order to prepare well balanced cold emission cathode with long stability, however too thin layer reduces cathode lifetime as it is bombarded by ions. The tunneling parameter E_T (equation 3) should be lowest as possible in order to reach low effective mass of the electrons which helps them to tunnel through the barrier. From the noise measurement (figs. 4 and 5.) we can identify the ions, bombarding the cathode surface, which proves itself by sudden burst noise. The bombardment reduces the epoxy layer which leads to its complete destruction after 1 - 10 days. The noise spectral density (where the 1/f noise prevails), changes to $1/f^n$, where n is located between 1 and 2. The higher the n is, the more significant G-R is.

ACKNOWLEDGEMENTS

This research has been partially supported by GACR No. P102/11/0995 and under the project MSM 0021630503.

REFERENCES

[1] S. M. Sze, Physics of Semiconductor Devices, Wiley-Interscience, New York, (1981).

[2] K. W. Boer, Survey of Semiconductor Physics, Van Nostrand Reinhold (1990).

[3] J. Sikula et al., Niobium Oxide and Tantalum Capacitors: Quantum Effects in Charge Carrier Transport; CARTS USA 2006, 421 – 427.

[4] C. M. Benjamin et al., A Study on the Capacitance-Voltage Characteristics of Metal-Ta2O5-Silicon Capacitors for VLSI MOS Gate Oxide Applications, J. Appl. Phys. 85 (1990), 4087.

[5] C. Chaneliere et al., Tantalum pentoxide (Ta2O5) thin films for advanced dielectric applications, Material Science and Eng., R22 (1998), 269-322

[6] C. A. Mead, “Electron transport mechanisms in thin insulating films”, Phys. Rev. 128 (1962), 088.

[7] A. J. Melmed, J., The art and science and other aspects of making sharp tips, Fifth international conference on scanning tunnelling microscopy/spectroscopy, Vol. 9, No. 2. (1991), p. 601-608.

[8] Z.Q. Yu, et al. Reproducible tip fabrication and cleaning for UHV STM. Ultramicroscopy [online]. 2008, s. 873-877.

[9] L. Eckertová, L. Frank, Methods of surface analysis - the electron microscopy and di_raction, chapt. 2(p. 68-77), chapt. 3(p. 84-89) Academia, Prague, 1996.

[10] O. L. Golubev, V. N. Shrednik, Heat-Field Treatment of Tips Made of Tungsten-Hafnium Alloy, Technical Physics Vol. 48, No. 6, 2003, pp. 776-779.

[11] I. Slaidins, Accuracy of Noise Measurements for 1/f and GR Noise, Advanced Experimental Methods For Noise Research in Nanoscale Electronic Devices, vol. 151, 271-278, Springer 978-1-4020-2169-5, ISBN: 978-1-4020-2169-5.

[12] N. S. Xu, H. S. Ejaz, Novel cold cathode materials and applications, Materials Science and Engineering: R: Reports, Volume 48, Issues 2-5, 31 January 2005, Pages 47-189, ISSN 0927-796X.